Original Article

Histological Study of the Possible Protective Action of Platelet Rich Plasma on the Injurious Effect Induced by Aluminum Chloride on Albino Male Rat Cerebellar Cortex

Essam M. Laag and Sadika M. Tawfik

Department of Histology, Tanta University, Faculty of Medicine, Egypt

ABSTRACT

Background: Aluminum compounds are commonly used in many human activities. They are used in pesticides, detergents, cosmetics, pharmaceuticals, and food additives. Many studies revealed a link between human exposure to aluminum and many neurodegenerative conditions in which there is platelet dysfunction.

Aim of the Study: The aim of this research was to study the potential protective effect of platelet rich plasma on the deleterious histological effect of aluminum chloride on male rat cerebellar cortex.

Materials and Methods: In this study, three equal groups of adult male albino rats were used; each consisted of 10 rats: group I a and I b (control group), group II (daily intraperitoneal injection of aluminum chloride dissolved in saline for 60 consecutive days in a dose of 10mg/kg) and group III were given PRP (subcutaneous injection in a dose of 0.5 ml/kg twice weekly) in addition to aluminum chloride in the same previous dose and duration. Cerebellum sections were processed for hematoxylin and eosin staining, GFAB staining and electron microscopic examination.

Results: Aluminum chloride administration resulted in many histological alterations. Glial fibrillary acidic protein-positive cells were significantly present in the cerebellum of aluminum chloride-treated animals relative to control animals. Purkinje cells with darkly stained ill-defined nuclei with dark vacuolated cytoplasm with dilated RER cisterns, swollen mitochondria with destroyed crista were observed in an ultrastructural study for the cerebellar cortex of the aluminum chloride-treated group. It also showed degenerated granule cells with the disappearance of the nuclear membrane and vacuolation of the cytoplasm. Some of the myelinated nerve fibers showed degenerative changes. Concomitant administration of PRP decreased these effects.

Conclusion: PRP partially minimized the severity of aluminum chloride-induced cerebellar cortex injurious histological effects in male albino rats. Further research is needed to extend these findings to clinical practice.

Received: 07 December 2020, **Accepted:** 19 January 2021

Key Words: Albino rat, aluminum, PRP.

Corresponding Author: Essam M. Laag, Department of Histology, Tanta University, Faculty of Medicine, Egypt, **Tel.**: +201 220488500, **E-mail:** emlaag@gmail.com

ISSN: 1110-0559, Vol. 44, No.4

INTRODUCTION

Aluminum compounds are commonly used in many human activities. These include aluminum hydroxide, chloride, nitrate, phosphate, silicate, sulphate, and potassium. They are used in pesticides, detergents, cosmetics, pharmaceuticals, and food additives.[1] A brain is a common place for aluminum toxicity because aluminum can cross the blood brain barrier.[2] Epidemiological and animal studies revealed that aluminum toxicity can lead to neuroinflammation and neuronal necrosis.[3] Recent studies indicated that aluminum is contained in brain tissue in autism, multiple sclerosis and Alzheimer's disease.[4]

Platelet rich plasma (PRP) is a product obtained by blood centrifugation which contains high platelet concentration in a small amount of plasma. It contains many growth factors, including vascular endothelial growth factor, transforming growth factor β1 & β2, platelet derived growth factor αα, αβ and ββ and epithelial growth factor.[5] Many studies have shown that the growth factors delivered by PRP can regulate the growth, differentiation, and survival of neurons in neurodegenerative diseases.[6]

AIM OF OUR WORK

This study was performed to study the potential protective effect of platelet rich plasma on the deleterious histological effect of aluminum chloride on the male rat cerebellar cortex.

MATERIALS AND METHODS

Animals

For this study, a group of thirty adult male albino rats was used. Their weight varied from 180 to 260 g. They were bought from the animal house of the National Research Center in Cairo, Egypt. They were kept in stainless steel cages under standard daylight/dark hours. Rats were left to acclimate for 2 weeks before the experiment. Free access to standard laboratory diet and water ad libitum was given to the animals. The rats had been maintained according to the guidelines for animal experiments approved by the Ethical Committee of the Faculty of Medicine, Tanta University, Egypt.

 DOI: 10.21608/ejh.2021.49889.1386

Experimental design

Three equal groups of rats were used; each group consisted of 10 rats:

- Group I (control) (10 rats): divided into 2 subgroups:
  - Subgroup I a (5 rats): did not receive any treatment.
  - Subgroup I b (5 rats): received daily intraperitoneal injection of 0.1 ml saline for 60 consecutive days.
- Group II (10 rats): received daily intraperitoneal injection of aluminum chloride (Al Cl3) (Sigma Chemical Company, St Louis, Missouri, USA) dissolved in saline for 60 consecutive days in a dose of 10mg/kg.[7]
- Group III (10 rats): received the same treatment as group II concomitant with subcutaneous injection of PRP (0.5 ml/kg) twice weekly.[8]

At the end of the experiments, all the rats were anesthetized with ether inhalation, perfused with 4% paraformaldehyde and scarified. The cerebellum was extracted and treated for histological, immunohistochemical and electron microscopic studies.

Preparation of PRP

The procedure was performed in the tissue culture lab in Histology Department, Faculty of Medicine, Tanta University. Donor animals were anesthetized by inhalation of ether and the blood was obtained by cardiac puncture. Using a sterile syringe that contains 0.3 ml of 3.8% sodium citrate, 2.5-3 ml of blood were obtained from each rat. 10 µl complete blood was collected to count the number of platelets by adding 2.5 ml platelet counting solution using hemocytometer. Then collected sample was then centrifuged for 7 minutes at 3000 rpm. The supernatant was aspirated by a micropipette. It was then poured into another sterile tube and centrifuged for 5 minutes at 4000 rpm. The supernatant was removed leaving only 1ml of the supernatant over the pellet. The pellet was then resuspended in the remaining supernatant. We then used 10 µl of the suspension for manual counting of the platelets. At this stage, the platelets were nearly 5 times the number counted in the complete blood sample. PRP was then activated by adding 0.1ml of calcium chloride to each ml.[9-11]. Immediately, 0.5 ml PRP was diluted by phosphate buffer saline (PBS) (PRP 1:1 PBS), placed in a sterile insulin syringe, and injected subcutaneously.[12]

Light microscopic examination

Samples were fixed in 10% neutral buffered formalin and 5µm thick sections were stained with hematoxylin and eosin.[13]

Immunohistochemical study for glial fibrillary acidic protein (GFAP)

For two days, sections were fixed in 10% neutral buffered formalin. They were then incubated with a monoclonal antibody for GFAP (Sigma, St Louis, Missouri, USA) and a technique involving modified avidin-biotin peroxidase (Thermo Scientific Co, Waltham, Massachusetts, USA) was applied to show the astrocytes as described previously[14] Negative control slides were obtained using the same technique, except that we used PBS instead of the primary antibody.

Quantitative evaluation of immune-stained sections

We used the image analyzer system Leica Qwin 500 (Solms, Germany) in the Central Research Laboratory at Tanta University College of Medicine. The optical density and the region percentage of the astrocyte GFAP composition in the granular, Purkinje, and cerebellum molecular layers were evaluated. Ten non overlapping fields at x400 magnification in 5 randomly selected sections from 5 animals in each group were used.

Statistical analysis

We used the SPSS program (SPSS Inc., Chicago, IL, USA) to analyze the data. ANOVA and Post Hoc test were applied and the results were displayed as mean values ± SD with significance level (*P-value*) 0.05.

Semithin sections and electron microscopic study

Small samples of the cerebellum were fixed in 2.5 % gluteraldehyde in 0.1 M phosphate buffered saline (pH 7.3) at 400 C for two hours. They were then rinsed in 0.1M phosphate buffered saline and postfixed in 1% osmium tetroxide in the same buffer for 1 h at 4°C, then dehydrated in ascending grades of ethanol. After immersion in propylene oxide, the specimens were embedded in embed-812 resin in BEEM capsules (Polyscience, Warrington, Pennsylvania, USA) at 60°C for 24 h. Semithin sections (1 µm thick) were cut using an ultramicrotome. They were stained with 1% toluidine blue. Ultrathin sections were cut using an ultramicrotome. They were then stained with uranyl acetate and lead citrate[15] to be examined by a JEOL electron microscope (Akishima, Tokyo, Japan) at 80 kV in Faculty of Medicine, Tanta University, Egypt.

RESULTS

Light microscopic results

The examination of the H&E and toluidine blue-stained pieces of the control group (I a and I b) demonstrated the standard configuration of the cerebellar cortex, consisting of the molecular layer, the granular layer and the Purkinje cell layer in between. The molecular layer was formed of scattered cells (small stellate cells located superficially and basket cells in the deeper parts near Purkinje cells) and fibers. The granular layer was formed of densely packed spherical cells having dark nuclei and clear spaces (cerebellar islands) where synapses occur. The Purkinje

cell layer consisted of large pyriform cells grouped in a single row at the molecular layer interface with the granular layer. These cells had distinct pale nuclei with conspicuous nucleoli surrounded by cytoplasmic Nissl granules (Figures 1,2). Examination of the aluminum chloride treated group (group II) indicated that the changes were significant clear in the Purkinje cell layer in the form of proliferation and multilayer deposition and invasion of the molecular layer. They were also widely separated, darkly stained and surrounded by unstained area. Cerebellar islands (glomeruli) were darkly stained and vacuolated. The other two layers were vacuolated and contained darkly stained nuclei (Figure 3). Some Purkinje cell bodies were shrunken with irregular shapes with dark cytoplasm and dark, hardly identifiable nucleus (Figure 4). Examination of group III (aluminum chloride and PRP) displayed less proliferation of Purkinje cells and mild vacuolation in the molecular layer (Figure 5). Some Purkinje cells looked nearly normal and others looked like those in the aluminum chloride treated group (Figure 6)

Immunohistochemical staining for Glial Fibrillary Acidic Protein (GFAP) revealed mild effective reaction in the processes and cytoplasm of astrocytes in control rats whereas this positive reaction was intense in aluminum chloride treated animals in the three cortical layers. Rats concomitantly treated with PRP (group III) displayed moderate reaction compared to aluminum chloride treated animals (Figures 7,8,9). The optical density and the area percentage of the GFAP content of the astrocytes in the three cerebellum layers demonstrated a statistically significant improvement in both parameters in the aluminum chloride treated group relative to the other two groups. The group treated concomitantly with PRP reported a significant improvement compared to the control group and a significant reduction compared to the aluminum chloride treated group (Table 1, Graphs 1,2).

Electron microscopic results

The investigation of ultrathin sections of the cerebellar cortex of control animals showed the standard structure of Purkinje cells showing euchromatic nucleus and prominent nucleolus with cytoplasm having mitochondria, cisternae of the rough endoplasmic reticulum and dispersed ribosomes in the cytoplasm (Figure 10). Granular cells in the granule cell layer had heterochromatic nuclei with little cytoplasm around (Figure 11). Some myelinated nerve fibers were seen. These observed myelinated nerve fibers reveal the compact lamellar shape of the myelin sheath. Their axoplasm contained mitochondria and microtubules (Figure 12).

The investigation of the cerebellar cortex of aluminum chloride treated animals revealed Purkinje cells having a darkly stained ill-defined nucleus with dark vacuolated cytoplasm having dilated cisternae of RER, swollen mitochondria with destroyed cristae. The surrounding neuropil is vacuolated (Figure 13). It also showed degenerated granule cells where a karyolitic nucleus is seen surrounded by a disintegrated cytoplasm in some cells or depleted vacuolated cytoplasm in other. The nearby myelinated axons were irregularly dilated with thinning of their myelin and rarefaction of their axoplasm (Figure 14). Some of the myelinated axons in the granular layer showed degenerative changes in the form of disorganized irregular outline, a decrease of the tight lamellar structure of the myelin layers and splitting. Other axons had disruption and vacuolated axoplasm (Figure 15). Examining group III animals (concomitant treatment with aluminum chloride and PRP) showed almost normal Purkinje cells but with dark cytoplasm (Figure 16). The granule cells were nearly normal, but some of them showed cytoplasmic vacuolation (Figure 17). Most of the myelinated nerve fibers in the granular layer preserved their normal structure, but some showed loss of compact lamellae structure and some splitting (Figure 18).

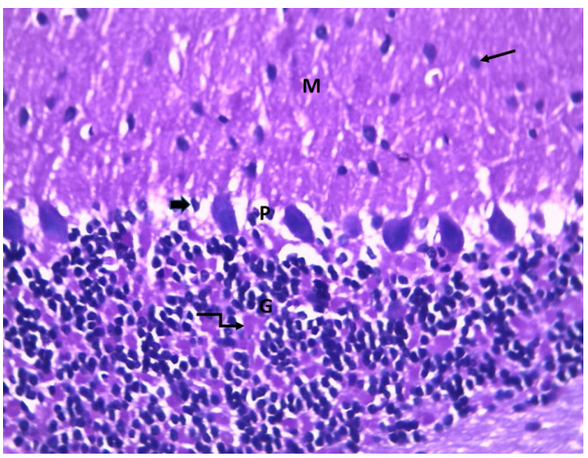

Fig. 1: A section of the cerebellar cortex of a control rat showing its three layers. The molecular layer (M) is consisting of superficial stellate cells (arrow) and basket cells located deeper near Purkinje cells (thick arrow). The Purkinje cell layer (P) is formed of one row of large pyriform cells. The granular layer (G) is formed of small rounded cells having darkly stained nuclei with cerebellar islands in between (right angle arrow). H&E, x400.

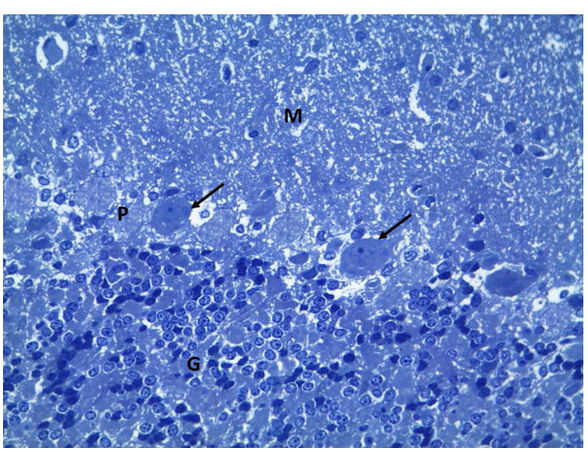

Fig. 2: A semithin section in the cerebellar cortex of a control rat showing large pyriform Purkinje cells having pale nucleus with prominent nucleolus surrounded by Nissl's granules (arrows). Toluidine blue, x400.

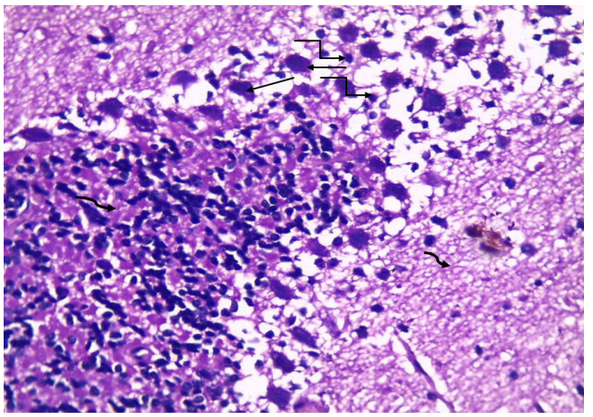

Fig. 3: A section of the cerebellar cortex of aluminum chloride-treated rat showing proliferation of Purkinje cells with multilayer deposition and invasion of the molecular layer. The cells are widely separated, darkly stained and surrounded by unstained area (arrows). Cerebellar islands (glomeruli) were darkly stained and vacuolated (right angel arrows). The other two layers were vacuolated and contained darkly stained nuclei (curved arrows). H&E, x400.

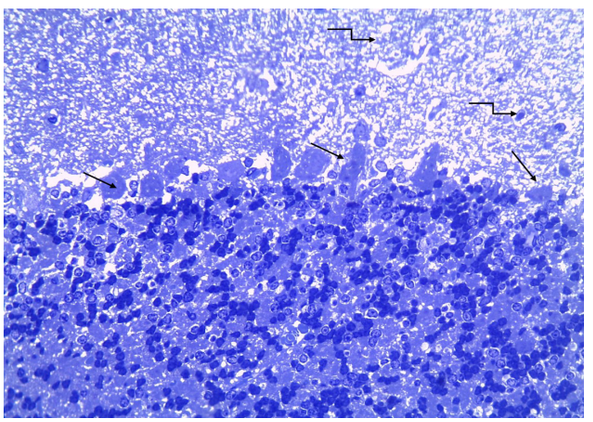

Fig. 4: A semithin section in the cerebellar cortex of aluminum chloride-treated rat showing some Purkinje cell bodies shrunken, having irregular shape with dark cytoplasm, and hardly identifiable nucleus (arrows). The molecular layer has highly vacuolated areas and contains few darkly stained disfigured cells (right angel arrows) Toluidine blue, x400.

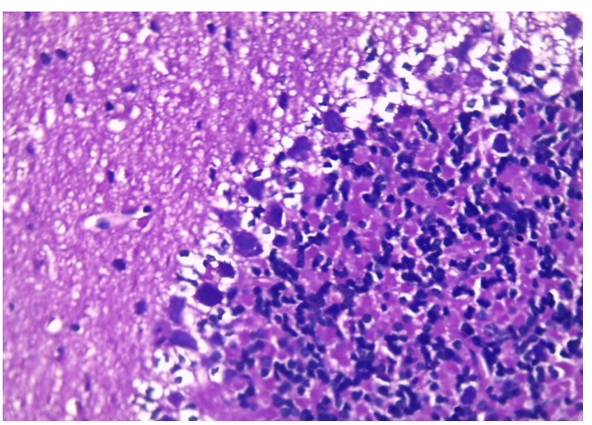

Fig. 5: A section of the cerebellar cortex of group IV (aluminum chloride and PRP) rats showing less proliferation of Purkinje cells compared to the aluminum chloride treated group. Molecular layer is mildly vacuolated compared to aluminum chloride treated group. H&E, x400.

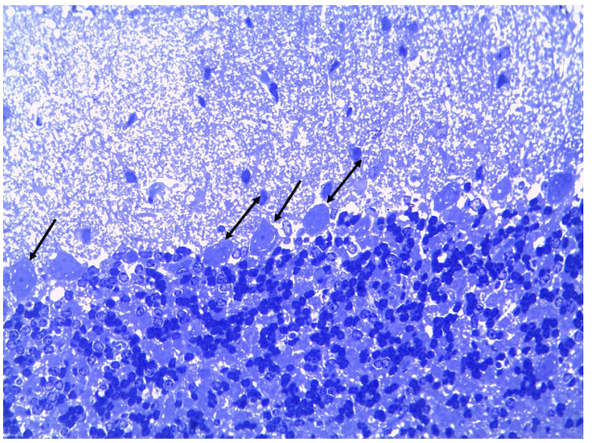

Fig. 6: A section of a semithin section in the cerebellar cortex of group IV (aluminum chloride and PRP) shows that some Purkinje cells look nearly normal (arrows) and others look like those in aluminum chloride treated group (double head arrows). Molecular layer is mildly vacuolated compared to aluminum chloride treated group. Toluidine blue, x400.

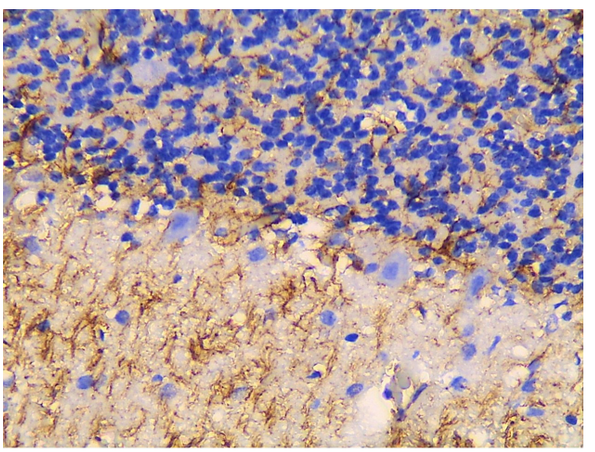

Fig. 7: A section of the cerebellar cortex of a control rat showing mild positive GFAP reaction in the processes and cytoplasm of astrocytes in the three cortical layers. GFAP immunostaining, x400.

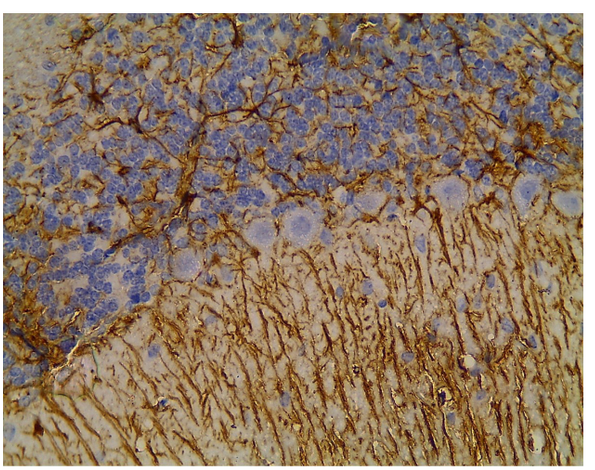

Fig. 8: A section of the cerebellar cortex of aluminum chloride-treated rat showing intense positive GFAP reaction in the processes and cytoplasm of astrocytes in the three cortical layers. GFAP immunostaining, x400.

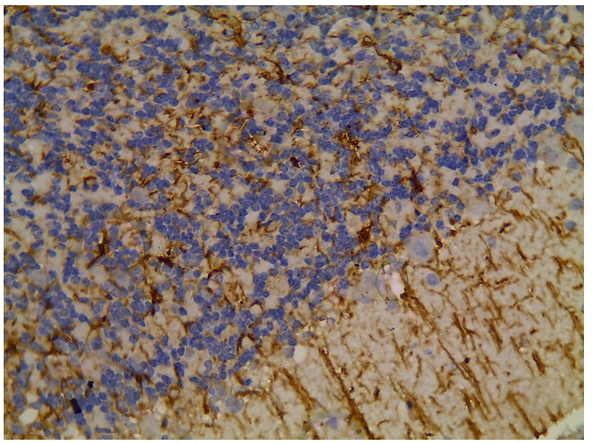

Fig. 9: A section of the cerebellar cortex of group IV (aluminum chloride and PRP) shows moderate GFAP reaction in the processes and cytoplasm of astrocytes in the three cortical layers compared to the aluminum chloride treated group. GFAP immunostaining, x400.

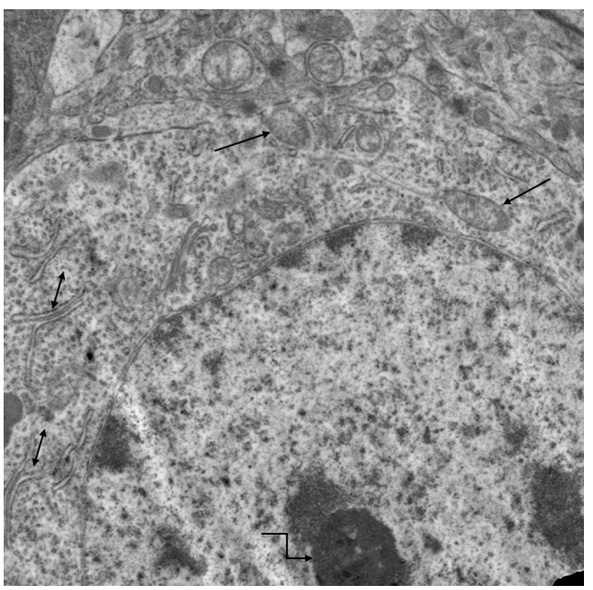

Fig. 10: An ultrathin section of the cerebellar cortex of control animal showing a part of a normal Purkinje cell revealing euchromatic nucleus with prominent nucleolus (right angle arrow), mitochondria (arrows), rough endoplasmic reticulum (double head arrows) and dispersed ribosomes in the cytoplasm. Mic. Mag., X6000.

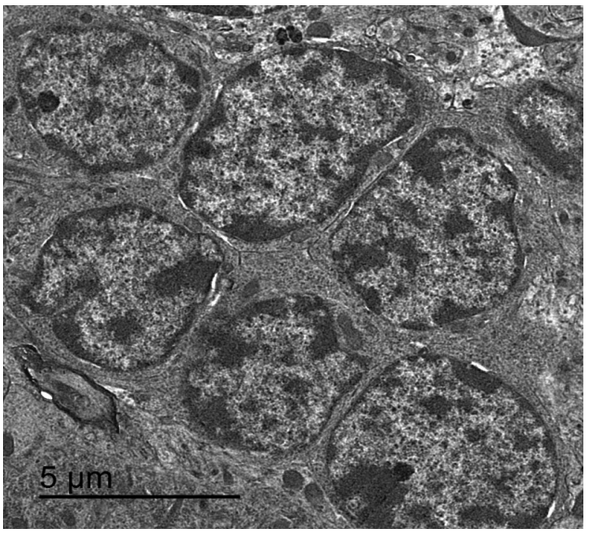

Fig. 11: An ultrathin section of the cerebellar cortex of control animal showing granule cells having heterochromatic nuclei with little cytoplasm around. Mic. Mag., x6000.

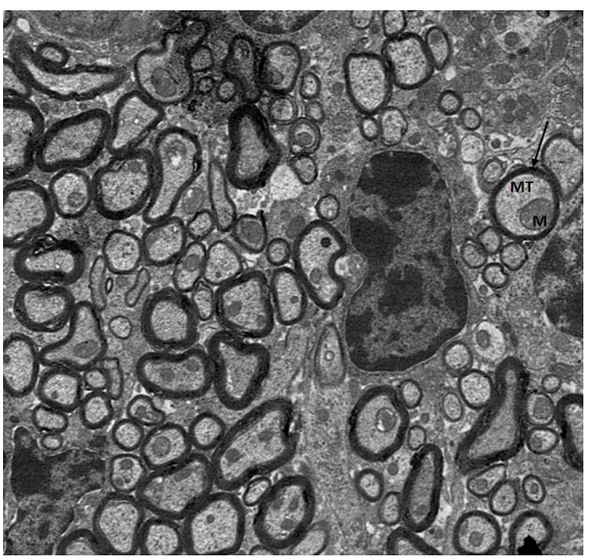

Fig. 12: An ultrathin section of the cerebellar cortex of control animal showing myelinated nerve fibers with compact lamellar structure of myelin sheath (arrow), mitochondria (M) and microtubules (MT) in their axoplasm. X2400.

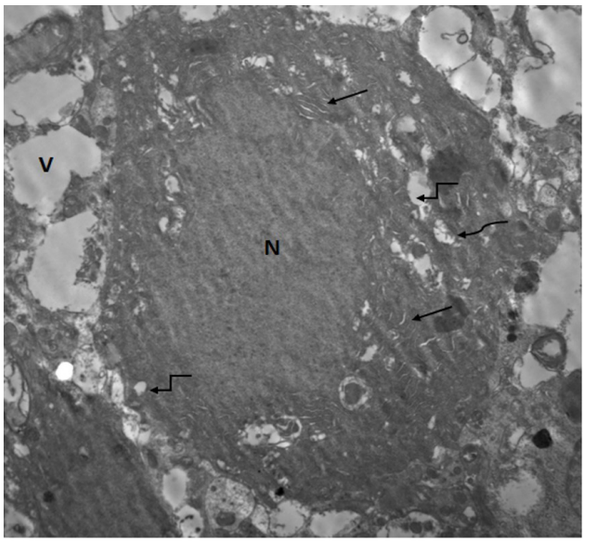

Fig. 13: An ultrathin section of the cerebellar cortex of aluminum chloride treated animal showing Purkinje cell having ill-defined darkly stained nucleus (N) with dark vacuolated cytoplasm (right angled arrows) that reveals dilated cisternae of RER (arrows) and swollen mitochondria with destroyed cristae (curved arrow). The surrounding neuropil is vacuolated (V). X2400.

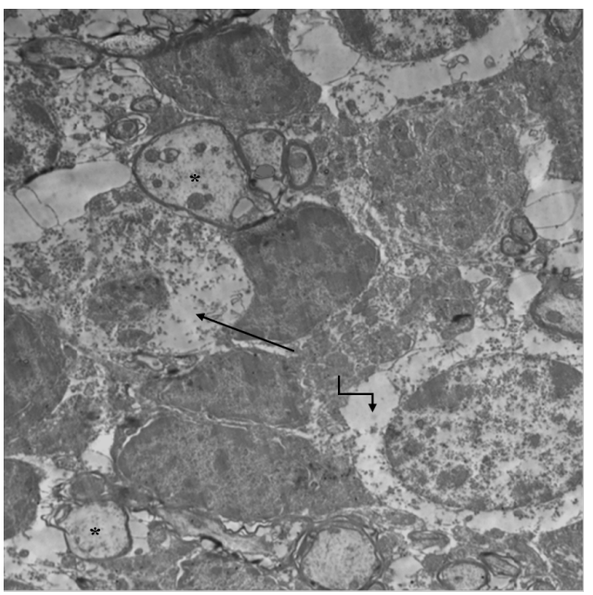

Fig. 14: An ultrathin section of the cerebellar cortex of aluminum chloride treated animal showing degenerated granule cells where a karyolitic nucleus is seen surrounded by a disintegrated cytoplasm (arrow) in some cells or depleted vacuolated cytoplasm in other (right angled arrow). The nearby myelinated axons are irregularly dilated with thinning of their myelin and rarefaction of their axoplasm (*). X2400.

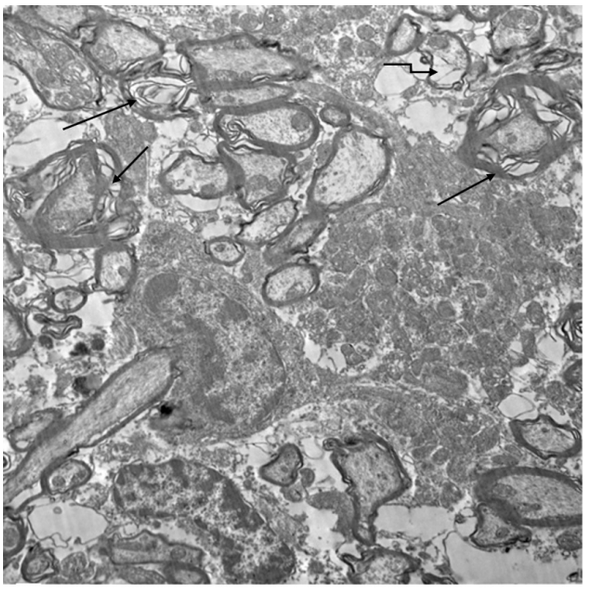

Fig. 15: An ultrathin section of the cerebellar cortex of aluminum chloride treated animal showing myelinated axons in the granular layer having disorganized irregular outline, loss of the lamellar compact structure of myelin layers and splitting (arrows). Some had vacuolated axoplasm and disruption of the myelin (right angled arrow). X2400.

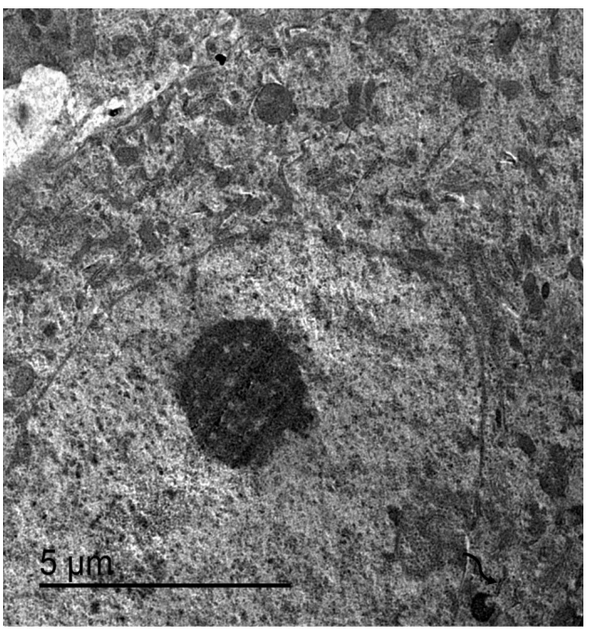

Fig. 16: An electron micrograph of the cerebellar cortex of group IV (aluminum chloride and PRP) shows almost normal Purkinje cell but with dark cytoplasm. Mic. Mag., x6000.

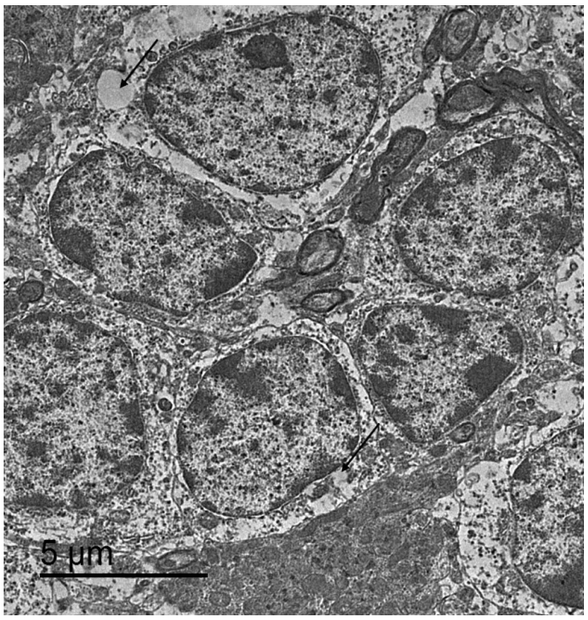

Fig. 17: An ultrathin section of the cerebellar cortex of group IV (aluminum chloride and PRP) shows nearly normal granule cells. Some of them show cytoplasmic vacuolation (arrows). Mic. Mag., x6000.

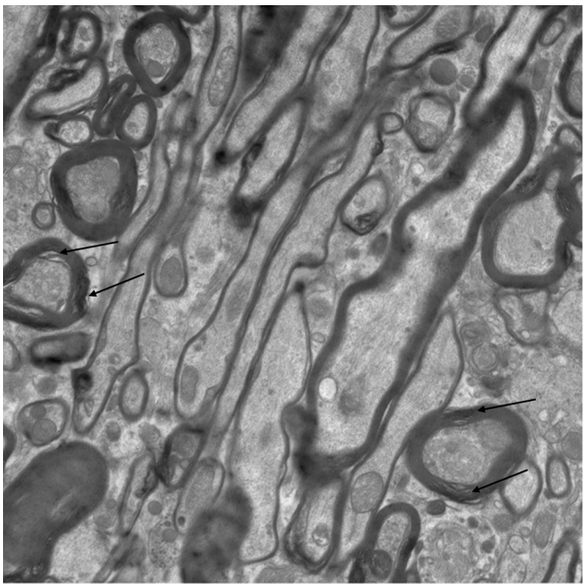

Fig. 18: An ultrathin section of the cerebellar cortex of group IV (aluminum chloride and PRP) shows that most of the myelinated nerve fibers in the granular layer are preserving their normal structure but some of them display loss of compact lamellar structure and splitting (arrows). X2400.

Table 1: Comparison between Mean Area Percentage and mean optical density in control group, Aluminum chloridw treated group, and Aluminum chloride plus PRP treated group

	Control (group 1)	Aluminum chloride treated (group 2)	Aluminum chloride treated + PRP (group 3)	*P - value*
Mean Area Percentage (mean ± SD)	15 ± 3.7	34.9 ± 2.9	22 ± 2.4	P < 0.001 P1 = 0.03 P2 = 0.02* P3 = 0.04**
Mean Optical density (mean ± SD)	0.11 ± 0.01	0.23 ± 0.02	0.16 ± 0.02	P < 0.001 P1 = 0.05 P2 = 0.02* P3 = 0.03**

P Significant for ANOVA
P1: Between groups 1 and 2
P2**: Between groups 1 and 3
P3***: Between groups 2 and 3
Comparison was done using ANOVA and Post Hoc test

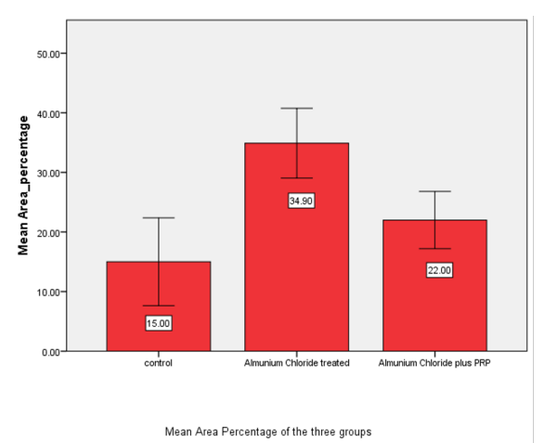

Graph 1: Mean area percentage for the three groups (control, aluminum chloride treated and aluminum plus PRP treated)

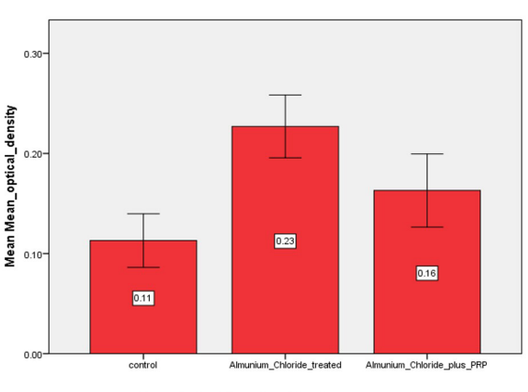

Graph 2: Mean optical density for the three groups (control, aluminum chloride treated and aluminum plus PRP treated)

DISCUSSION

Aluminum is widely found in the environment and food. Exposure to this metal is nearly impossible to avoid[16] It is highly neurotoxic and causes degeneration of nerve cells in the brain of human and experimental animals.[17]

In our study, aluminum exposure resulted in multilayer deposition of Purkinje cells and invasion of the molecular layer. Some Purkinje cell bodies were shrunken having irregular shape with dark cytoplasm, and dark hardly identifiable nucleus. Both molecular and granular layer showed vacuolation. The multilayer deposition might be explained by the fact that prolonged aluminum exposure caused neuronal injury. The Purkinje cells attempted to adapt by crowding in a test to re-establish synaptic connection with other neurons to fulfill their function. The shrinking, dark nucleoplasm and cytoplasm can reflect a specific degree or state of apoptosis.[18,19] This agreed with previous reports indicating that aluminum exposure induces neuronal apoptosis.[20] The vacuolation showed within the molecular and granular cell layers were attributed by some authors to spongiform changes and by others to loss of the cellular components within the cerebellar cortex.[21]

Our study revealed a significant increase in GFAP immunoreaction in the astrocyte's cell body and processes in the aluminum chloride treated group relative to the control group. Intermediate filaments are a fundamental cytoskeletal component in neurons and astrocytes. GFAP is considered the fundamental intermediate filament in astrocytes. GFAP is a crucial element in preserving the architecture of the astrocytes. It is also responsible for the support of the physiology of the nearby neurons. It is implicated in the pathology of several neurological diseases. Its overexpression is a marker of astrogliosis in many neurological diseases.[22] The astrogliosis reaction may be considered as a compensatory mechanism to deal with neurodegeneration. The activated astrocytes play a crucial role in tissue repair after neuronal insult.[23]

Ultrastructural examination of aluminum chloride treated animals showed that Purkinje cells had darkly stained ill-defined nucleus with dark vacuolated cytoplasm having dilated cisternae of RER, swollen mitochondria with destroyed cristae. The surrounding neuropil was vacuolated. Zimatkin and Bon indicated that hyperchromic dark neurons are cells that are active in protein synthesis intensely exposed to unfavorable factors for a prolonged period leading to their death by apoptosis.[24] Cytoplasmic vacuolation was considered by some researchers to be a type of hydropic degeneration.[25] The dilated cisternae of RER and the swollen mitochondria with destroyed cristae might be attributed to increased oxidative stress induced by aluminum exposure which is known to have prooxidant activity leading to an increase in intracellular reactive oxygen species (ROS).[26] The polyunsaturated fatty acids in the biological membranes can be attacked by ROS releasing free oxygen radicals.[27] Free radicals induce lipid peroxidation and protein fragmentation, causing membrane and organelle damage.[28] This will lead to an increase in plasma membrane permeability to sodium. Sodium accumulation causes an increase in water content and swelling[29], inducing damage and dilatation of the organelles. The surrounding neuropil vacuolation might be caused by shrinkage of Purkinje cell bodies and the withdrawal of their processes.[30]

Our electron microscopic study showed that some granule cells in group III (aluminum chloride treated) degenerated with vacuolated cytoplasm. This was in accordance with previous studies showing that granule cells were a particular target for aluminum neurotoxicity.[31] Some of the myelinated axons in the same group (group III) showed degenerative changes in the form of disorganized irregular outline, loss of the tight lamellar structure of the myelin layers and splitting. Other axons had disruption and vacuolated axoplasm. Aluminum can initiate lipid and protein oxidation in brain myelin and synaptic membranes promoting oxidative damage. This makes myelin a preferred target of aluminum-induced oxidative damage[32] Disruption of myelination was due to changes in the essential protein of myelin after exposure to the toxic material. Absence of the lamellar compact structure of the myelin layers and separation was also associated with higher water content due to nerve degeneration that leads to edema in the myelin sheath contributing to the splitting of myelin lamellae.[33]

In this work, the concomitant administration of PRP minimized the toxic effects of AL on the cerebellum. Given their captivating capacity to store, produce and deliver particular subsets of bioactive particles, including molecules involved in paracrine signaling and neurochemicals that transmit nerve impulses across synapses, platelets can play a crucial role in maintaining healthy brain physiology. Various neurodegenerative conditions are now known to have platelet disorder as part of their pathology, underscoring the therapeutic importance of PRP.[34] One important example of these neurodegenerative conditions is Alzheimer's disease in which there is increased platelet secretase activity[35,36] and platelet-mediated amyloid- beta aggregation.[37,38] Many studies revealed a link between human exposure to aluminum and Alzheimer's disease[39] Other neuro-degenerative conditions that are linked to aluminum exposure and have platelet dysfunction include: Parkinson's disease (increased platelet mHtt protein,[40] increased platelet aspartate and glycine uptake[41,42]), and multiple sclerosis (platelet mediated neuroinflammation in the spinal cord and the hippocampus[43-45]).

CONCLUSION

Aluminum chloride exposure induced injurious histological effects in the cerebellar cortex of male albino rats. Concomitant administration of platelet rich plasma partially minimized the severity of these injurious effects. Further research is needed to extend the application of these findings in clinical practice.

CONFLICT OF INTERESTS

There are no conflicts of interest.

REFERENCES

1. Igbokwe I, Igwenagu, E, Igbokwe N. (2019). Aluminium toxicosis: a review of toxic actions and effects. Interdisciplinary toxicology; 12(2): 45–70.
2. Zhao Y, Dang M, Zhang W, *et al*. (2020). Neuroprotective effects of Syringic acid against aluminium chloride induced oxidative stress mediated neuroinflammation in rat model of Alzheimer's disease. Journal of Functional Foods; 71: 104009.
3. Cheng X, Gu J, Pang Y, Liu J, *et al*. (2019). Tacrine-hydrogen sulfide donor hybrid ameliorates cognitive impairment in the aluminium chloride mouse model of Alzheimer's disease. ACS Chemical Neuroscience; 10 (8): 3500-3509.
4. Exley C, Clarkson E. (2020). Aluminium in human brain tissue from donors without neurodegenerative disease: A comparison with Alzheimer's disease, multiple sclerosis, and autism. Sci Rep; 10: 7770.
5. Luzo A, Fávaro W, Seabra A, *et al*. (2020). What is the potential use of platelet-rich-plasma (PRP) in cancer treatment? A mini review. Heliyon; 6 (3): e03660.
6. Chen N, Sung C, Wen Z, *et al*. (2018). Therapeutic Effect of Platelet-Rich Plasma in Rat Spinal Cord Injuries. Front. Neurosci.; 1:12.
7. Shuchang H, Qiao N, Piye N, *et al*. (2009). Protective effects of gastrodia elata on aluminium-chloride-induced learning impairments and alterations of amino acid neurotransmitter release in adult rats. Restor Neurol Neurosci; 26:467–473.
8. El-Tahawy F, Rifaai A, Saber A, *et al*. (2017). Effect of Platelet Rich Plasma (PRP) Injection on the Endocrine Pancreas of the Experimentally Induced Diabetes in Male Albino Rats: A Histological and Immunohistochemical Study. J Diabetes Metab 8: 730.
9. Quarteiro L, Tognini F, Flores de Oliveira L, *et al*. (2015). The effect of platelet-rich plasma on the repair of muscle injuries in rats. Rev Bras Ortop; 50(5): 586–95.
10. Kim H, Je J, Kim D, *et al*. (2011). Can platelet rich plasma be used for skin rejuvenation. Evaluation of effects of platelet rich plasma on human dermal fibroblast. Ann Dermatol, 23: 424-31.
11. Mary Lou, T. Clinical hematology - theory and procedures, 5th edition. Lippincott Williams Wilkins, Philadelphia, PA; 2011. pp. 320
12. Hesami Z, Jamshidzadeh A, Ayatollahi M, *et al*. (2014). Effect of Platelet-Rich Plasma on CCl 4 -Induced Chronic Liver Injury in Male Rats. International Journal of Hepatology 14: 1-7.
13. Bancroft J and Layton C (2018): The hematoxylins and eosin and Connective and other mesenchymal tissues with their stains in Bancroft's Theory and Practice of Histological Techniques. Survana SK Layton C and Bancroft J.D. 8th ed., Elsevier Health Sciences. pp: 126-137 and 166-169.
14. Saad EL-Dien H, EL Gamal D, Mubarak H, *et al*. (2010). Effect of fluoride on rat cerebellar cortex: light and electron microscopic studies. Egypt J Histol. 2010; 33:245–256.
15. Woods AE and Stirling JW (2018): Transmission electron microscopy in Bancroft's Theory and Practice of Histological Techniques. Survana SK Layton C and Bancroft J.D. 8th ed., Elsevier Health Sciences. pp: 434-449.
16. Mesole S, Alfred O, Yusuf U, *et al*. (2020). Apoptotic Inducement of Neuronal Cells by Aluminium Chloride and the Neuroprotective Effect of Eugenol in Wistar Rats. Oxid Med Cell Longev. 2020:8425643.
17. Bekhedda H, Menadi N, Demmouche A, *et al*. (2020). Histological study of the effects of aluminum chloride exposure on the brain of wistar rats female. Journal of Drug Delivery and Therapeutics; 10(3-s): 37-42.
18. Iwanowski L. (1988). Apoptosis and dark neurons. Neuropatol Pol; 26:573–579.
19. Ratan R, Murphy T, Baraban JM. (1994). Oxidative stress induces apoptosis in embryonic cortical neurons. J Neurochem; 62:376–379.
20. Zhang Q. (2018). Aluminum-Induced Neural Cell Death. Adv Exp Med Biol.; 1091:129-160.
21. Kassab A. (2018). Wheat germ oil attenuates deltamethrin-induced injury in rat cerebellar cortex: Histological and immunohistochemical study. Egyptian Journal of Histology; 41(2) 182-191.
22. McKeon A, and Benarroch E. (2018). Glial fibrillary acid protein Functions and involvement in disease. Neurology; 90 (20): 925-930.
23. Kassab A. (2018). Wheat germ oil attenuates deltamethrin-induced injury in rat cerebellar cortex: Histological and immunohistochemical study. Egyptian Journal of Histology; 41(2) 182-191.
24. Zimatkin M, and Bon I. (2018). Dark Neurons of the Brain. Neurosci Behav Physi; 48: 908–912.
25. Krinke J. (2011). Neuronal Vacuolation. Toxicologic Pathology; 39(7):1140-1140.
26. Deiaa El-Din M, EL–Shafeia M, Kamel A, *et al*. (2011). Effect of aluminum on the histological structure of rats' cerebellar cortex and possible protection by melatonin. Egypt J Histol; 34:239–250.
27. Mate´s M, Pe´rez-Go´mez C, and Nu´n˜ez de Castro I. (1999). Antioxidant enzymes and human diseases. Clin Biochem; 32:595–603.

28. Kumar V, Abbas A, and Fausto N. (2008): Robbins and Cotran Pathologic Basis of Disease. 7th edition, Elsevier Saunders, Philadelphia, Pennsylvania (USA). Chap. 1, Cellular adaptation, cell injury and cell death. P: 3.

29. Emanuel R. (2001): Essential Pathlogy. 3rd edition, Lippincot Williams & Wilkins, Baltimore, MD (USA). Chap. 1, Cell injury. P:1.

30. Afifi O. (2009). Effect of Sodium Fluoride on the Cerebellar Cortex of Adult Albino Rats and the Possible Protective Role of Vitamin B6: A Light and Electron Microscopic Study. Egypt. J. Histol.; 32(2): 81-90.

31. Rodella L, Rezzani R, Lanzi R, *et al*. (2001). Chronic exposure to aluminium decreases NADPH-diaphorase positive neurons in the rat cerebral cortex. Brain Res; 889:229–233.

32. Verstraeten V, Golub S, Keen L, *et al*. (1997) Myelin is a preferential target of aluminum-mediated oxidative damage. Arch Biochem Biophys; 344(2):289-94.

33. Manzo L, Artigas F, Martinez E, *et al*. (1996): Biochemical markers of neurotoxicity. A review of mechanistic studies and applications. Hum.Exp. Toxicol.; Suppl 1:S20-S35.

34. Leiter O, & Walker L. (2020). Platelets in Neurodegenerative Conditions-Friend or Foe. Frontiers in immunology; 11; 747.

35. Johnston A, Liu W, Coulson R, *et al*. (2008). Platelet β-secretase activity is increased in Alzheimer's disease. Neurobiol Aging; 29:661–68.

36. Liu W, Todd S, Craig D, *et al*. (2008). Elevated platelet ß-secretase activity in mild cognitive impairment. Dement Geriatr Cogn Disord; 24:464–8.

37. Donner L, Fälker K, Gremer L, *et al*. (2016). Platelets contribute to amyloid-β aggregation in cerebral vessels through integrin αIIbβ3-induced outside-in signaling and clusterin release. Sci Signal; 9:ra52.

38. Kniewallner M, Foidl M, Humpel C. (2018). Platelets isolated from an Alzheimer mouse damage healthy cortical vessels and cause inflammation in an organotypic ex *vivo* brain slice model. Sci Rep; 8:15483.

39. Mold M, Linhart C, Gómez-Ramírez J, *et al*. (2020). Aluminum and Amyloid-β in Familial Alzheimer's Disease. J Alzheimers Dis; 73(4):1627-1635.

40. Denis L, Lamontagne-Proulx J, St-Amour I, *et al*. (2019). Platelet abnormalities in Huntington's disease. J Neurol Neurosurg Psychiatry; 90:272–83.

41. Reilmann R, Rolf H, Lange W. (1997). Huntington's disease: N-methyl-d-aspartate receptor coagonist glycine is increased in platelets. Exp Neurol; 144:416–9.

42. Reilmann R, Rolf LH, Lange HW. (1994). Huntington's disease: The neuroexcitotoxin aspartate is increased in platelets and decreased in plasma. J Neurol Sci; 127:48–53.

43. Kocovski P, Jiang X, D'Souza S, *et al*. (2019). Platelet depletion is effective in ameliorating anxiety-like behavior and reducing the pro-inflammatory environment in the hippocampus in murine experimental autoimmune encephalomyelitis. J Clin Med; 8:162.

44. Langer F, Choi Y, Zhou H, *et al*. (2012). Platelets contribute to the pathogenesis of experimental autoimmune encephalomyelitis. Circ Res; 110:1202–10.

45. D'Souza Sonia C, Li Z, Luke Maxwell D, *et al*. (2018). Platelets drive inflammation and target gray matter and the retina in autoimmune-mediated encephalomyelitis. J Neuropathol Exp Neurol; 77:567–76.

الملخص العربى

دراسة هستولوجية للأثر الوقائى المحتمل للبلازما الغنية بالصفائح الدموية على التأثير التدميرى المستحدث لكلوريد الألومنيوم على قشرة المخيخ فى ذكر الجرذ الأبيض

عصام محمود لعج وصديقة محمد توفيق

قسم الهستولوجيا-كلية الطب ـ جامعة طنطا، مصر

مقدمة: يشيع استخدام مركبات الألومينيوم فى العديد من الأنشطة البشرية حيث يتم استخدامهم فى المبيدات الحشرية والمنظفات ومستحضرات التجميل والأدوية والمواد المضافة للأطعمة. هذا وقد أظهرت العديد من الدراسات وجود رابط بين التعرض البشرى للألومينيوم والعديد من حالات تحلل الجهاز العصبى التى يصاحبها اختلال فى وظائف الصفائح الدموية.

هدف الدراسة: أجريت هذه الدراسة لبحث الأثر الوقا ئى المحتمل للبلازما الغنية بالصفائح الدموية على التأثير التدميرى الهستولوجى المستحدث لكلوريد الألومينيوم على قشرة المخيخ فى ذكر الجرذ الأبيض البالغ.

مواد وطرق البحث: استخدم فى هذه الدراسة ثلاثون جرذا من الذكور البيضاء البالغة وتم تقسيمهم إلى أربع مجموعات: مجموعة ١و٢ (مجموعة ضابطة) ومجموعة ثالثة تم حقنها يوميا فى التجويف البريتونى بكلوريد الألومينيوم المذاب فى محلول الملح لمدة ستين يوما متتابعا بجرعة بلغت ١٠ميلليجرام لكل كيلوجرام ومجموعة را بعة حقنت بالبلازما الغنية بالصفائح الدموية تحت الجلد مرتين أسبوعيا بجرعة بلغت ٠,٥ ملليلتر لكل كجم بالإضافة إلى كلوريد الألومينيوم بنفس الجرعة والزمن المستخدم فى المجموعة الثالثة. وجهزت شرائح هستولوجية من المخيخ لصباغتها بالهيماتوكسيلين والإيوسين والبروتين الحمضى الدبقى الليفى وحضرت عينات للفحص بالميكروسكوب الإلكترونى. الهستولوجية

النتائج: أدى حقن كلوريد الألومينيوم إلى العديد من التغيرات الهستولوجية. ولوحظ عدد اكبر من الخلايا الموجبة التفاعل مع البروتين الحمضى الدبقى الليفى فى قشرة المخيخ للمجموعة المعالجة بكلوريد الألومينيوم مقارنة بحيوانات المجموعة الضابطة. وقد أظهر الفحص بالميكروسكوب الإلكترونى وجود خلايا بيركنجى بنواة داكنةغير واضحة المعالم وسيتوبلازم داكن به تجويفات واتساع فى الشبكة الإندوبلازمية االمحببة ووجود تمدد فى تمدد فى الميتوكوندريا مصحوبا بتدمير الأعرا ف. وقدأظهر أيضا وجود تحلل فى الخلايا المحببة مع اختفاء الغلاف النووى ووجود فجوات سيتوبلازمية. كما أظهر وجود تحلل فى بعض الألياف العصبية المحاطة بالميلين.وقد أدى الحقن المتزامن للبلازما الغنية بالصفائح الدموية مع كلوريد الألومينيوم إلى تقليل هذه التغيرات.

الإستنتاج: يؤدى الحقن المتزامن للبلازما الغنية بالصفائح الدموية إلى تقليل جزئي للآثار التدميرية الهستولوجية المستحدثة لكلوريد الألومينيوم علي القشرة المخيخية لذكر الجرذ الأبيض البالغ. ويجب إجراء المزيد من الأبحاث لكى يتم الاستفادة من نتائج البحث فى الممارسة الإكلينيكية